PROCEEDINGS OF SCIENCE

The QCD confining string and the worldsheet axion

Andreas Athenodorou[a,*]

[a] *Computation-based Science and Technology Research Center, The Cyprus Institute, Cyprus, 20 Konstantinou Kavafi Street, Aglantzia 2121*

E-mail: a.athenodorou@cyi.ac.cy

Recent findings from an extensive investigation of the flux tube spectrum and its implications for the axion on the worldsheet of the confining string are presented. Specifically, the latest results for both closed and open flux tubes in 4D $SU(N_c)$ gauge groups are discussed. For the closed flux tube, employing the thermodynamic Bethe ansatz (TBA) method with certain approximations, it is confirmed that a significant portion of the low-lying energy states, characterized by different sets of quantum numbers, can be effectively described by the low-energy effective theory of a long string consisting of two Goldstone bosons, known as phonons, along with a massive pseudoscalar referred to as the worldsheet axion. Regarding the open flux tube, recent findings indicate that a substantial portion of the excited states can be adequately approximated by the Nambu-Goto (NG) spectrum. However, deviations from the NG spectrum are observed in certain states, suggesting the presence of massive excitations. Notably, the mass of one of these excitations aligns with that extracted for the closed flux tube.

The XVIth Quark Confinement and the Hadron Spectrum Conference (QCHSC24)
19-24 August, 2024
Cairns Convention Centre, Cairns, Queensland, Australia

*Speaker

 ISSN 1824-8039 . Published by SISSA Medialab.

PoS(QCHSC24)044

1. Introduction

In confining gauge theories like $SU(N_c)$ gluodynamics, color charges generate flux tubes, forming what are known as confining strings. The dynamics of these flux tubes play a crucial role in our understanding of color confinement. By examining the excitation spectra of both *closed* and *open* flux tubes, we can gain valuable insights into the underlying mechanisms of confinement.

Over the past two decades, substantial progress has been made in understanding the effective string theory for the closed flux tube. Model-independent analyses based on lattice data have revealed a rich structure in the worldsheet dynamics, including the identification of multiple string-like states and a massive excitation known as the *worldsheet axion* [1, 2]. These findings suggest a complex interplay between Goldstone modes and additional degrees of freedom on the closed string worldsheet, with implications for both low-energy effective theories and high-energy behavior.

However, similar investigations have not yet been conducted for the open flux tube. The spectrum of open flux tubes presents challenges, including the impact of boundary conditions and potential differences in worldsheet degrees of freedom. Extending the analysis to open flux tubes in the large-N_c limit, offers an opportunity to assess whether features like the worldsheet axion are also present in the open strings and to explore defferences between open and closed string spectra.

In these proceedings, we present what is known for the closed and open flux tube spectra. First, we review the effective string theoretical framework for flux tubes and summarize recent findings. Followingly, we present the results from the TBA analysis for the closed flux tube. We then turn to the open flux tube, where we investigate its spectrum and the possible existence of axions on its worldsheet. By comparing the closed and open cases, we aim to build a comprehensive understanding of flux tube dynamics across different configurations, shedding light on the role of additional degrees of freedom in confining strings.

2. Effective Theory of Long Strings

Long strings, described by translational Goldstone bosons with non-linearly realized Poincaré symmetry, have low-energy excitations that can be captured by the effective action

$$S = -\int d^2\sigma \sqrt{-\det h_{\alpha\beta}} \left[\ell_s^{-2} + \gamma \ell_s^2 \mathcal{R}^2 + \dots\right], \tag{1}$$

where $\ell_s^{-2} = \sigma$ is the string tension, γ is a Wilson coefficient, and $\mathcal{R}$ is the scalar curvature. The first non-universal correction appears at $O(\ell_s^2)$, making the Nambu–Goto action, which manifests as the first term in the parenthesis, sufficient for universal predictions up to one-loop order.

For closed strings compactified on a circle of circumference R, the perturbative ℓ_s/R expansion can be used to calculate the torelon spectrum. While the leading non-universal contribution scales as ℓ_s^6/R^7 for long strings, lattice simulations show that many torelon states align well with the GGRT (Goddard-Goldstone-Rebbi-Thorn) spectrum [3, 4]:

$$E_{\rm GGRT}(N_L, N_R) = \sqrt{\frac{4\pi^2(N_L - N_R)^2}{R^2} + \frac{R^2}{\ell_s^4} + \frac{8\pi}{\ell_s^2}\left(\frac{N_L + N_R}{2} - \frac{D-2}{24}\right)}, \tag{2}$$

where N_L and N_R the contribution of left and right moving phonons in the energy respectively.

For open strings with length R with fixed boundaries, quantizing the Nambu-Goto action of Equation 1 up to leading order in ℓ_s^{-2}, yields the energy spectrum of an open relativistic string of length R with fixed endpoints. The resulting spectrum is given by the Arvis potential [5]:

$$E_N^{\rm NG}(R) = \sqrt{\frac{R^2}{\ell_s^4} + \frac{2\pi}{\ell_s^2}\left(N - \frac{D-2}{24}\right)}, \tag{3}$$

where N is the total contribution of the phonons with positive and negative circular polarizations.

The above expressions capture the relativistic corrections to the string's energy and illustrate how the interplay between the string tension and quantum fluctuations determines its behavior at both classical and quantum levels. The factor $\frac{D-2}{24}$ accounts for the zeroth-energy contributions of the $D-2$ transverse Goldstone bosons, reflecting the string's quantum nature in D-dimensional spacetime. The Weyl anomaly suggests that, at first glance, the Nambu-Goto energy prediction does not preserve Lorentz invariance, raising challenges in interpreting the confining flux tube within this framework.

2.1 Lorentz-Invariant Effective String Theories

The systematic study of Lorentz-invariant Effective String Theory (EST), which models the confining string, was pioneered by Lüscher, Symanzik, and Weisz in Ref. [6] through the static gauge approach, and later by Polchinski and Strominger in Ref. [7] using the conformal gauge. These methods allow for the derivation of the energy spectrum of string states as an expansion in powers of $1/(R\ell_s^{-1})$. In particular, contributions of order $O(1/R^p)$ originate from $(R+1)$-derivative terms in the EST action, with coefficients that initially appear as unconstrained Low Energy Coefficients (LECs). However, subsequent studies revealed that these LECs are subject to strict constraints imposed by the non-linear realization of Lorentz symmetry [8–10], leading to parameter-free predictions for specific terms in the $1/R$ expansion.

Different EST formulations arise from distinct choices of gauge fixing for the world-sheet embedding coordinates. The two dominant approaches are the *static gauge* [6, 8, 10] and the *conformal gauge* [7, 11, 12], both of which ultimately yield identical physical outcomes.

At the core of EST is the leading-order area term in 4, dictating the long-string behavior and producing a linearly increasing potential, is expressed as $E \simeq R/\ell_s^2$. The next-to-leading term in 4, derived from the Gaussian action, results in the well-known Lüscher correction, proportional to $1/R$, with a universal coefficient dependent solely on the spacetime dimension D.

$$S_{EST} = \ell_s^{-2} RT + \frac{\ell_s^{-2}}{2}\int \mathrm{d}^2x \partial_\alpha X_i . \partial^\alpha X^i + \frac{\ell_s^{-2}}{2}\int \mathrm{d}^2x \left(\frac{1}{8}(\partial_\alpha X_i . \partial^\alpha X^i)^2 - \frac{1}{4}(\partial_\alpha X_i . \partial^\beta X^i)^2\right) + \dots \tag{4}$$

The above four-derivative term introduces a correction of order $1/R^3$ with a universal coefficient dependent on D. Extending this analysis to six-derivative contributions [13, 14], one finds that in $D=3$, the correction remains universal and scales as $1/R^5$. However, in $D=4$, while the ground-state correction retains universality, excited-state corrections at order $O(1/R^5)$ do not. The $1/R$ expansion for the case of the closed flux tube leads to the expression:

$$E_n(R) = \ell_s^{-1}(R\ell_s^{-1}) + \frac{4\pi\ell_s^{-1}}{(R\ell_s^{-1})}\left(n - \frac{D-2}{24}\right) - \frac{8\pi^2\ell_s^{-1}}{(R\ell_s^{-1})^3}\left(n - \frac{D-2}{24}\right)^2 + \frac{32\pi^3\ell_s^{-1}}{(R\ell_s^{-1})^5}\left(n - \frac{D-2}{24}\right)^3 + \left(\frac{1}{(R\ell_s^{-1})^7}\right) \tag{5}$$

Unlike closed flux tubes, open flux tubes necessitate the inclusion of boundary terms [13, 14]. The energy spectrum for an extended open string follows the series expansion in $1/R$:

$$\begin{aligned} E_n(R) &= \ell_s^{-1}(R\ell_s^{-1}) + \frac{\pi\ell_s^{-1}}{(R\ell_s^{-1})}\left(n-\frac{D-2}{24}\right) - \frac{\pi^2\ell_s^{-1}}{2(R\ell_s^{-1})^3}\left(n-\frac{D-2}{24}\right)^2 + \frac{\bar{b}_2\pi^3\ell_s^{-1}}{(R\ell_s^{-1})^4}\left(B_n - \frac{D-2}{60}\right) \\ &+ \frac{\pi^3\ell_s^{-1}}{16(R\ell_s^{-1})^5}\left(n-\frac{D-2}{24}\right)^3 + \frac{\pi^3\ell_s^{-1}(D-26)}{48(R\ell_s^{-1})^5}C_n + \left(\frac{1}{(R\ell_s^{-1})^6}\right). \end{aligned} \tag{6}$$

In the above equation, $\bar{b}_2$ is a universal coefficient independent of the excitation number N, while B_N and C_N are state-dependent. In both equations above, the leading term, together with terms scaling as $1/(R\ell_s^{-1})$, $1/(R\ell_s^{-1})^3$, and $1/(R\ell_s^{-1})^5$ without inlcuding the boundary terms, align with the expansion of square root in both Equations 2 and 3 up to $O(1/(R\ell_s^{-1})^7)$. This implies that the Nambu-Goto equation represents a specific resummation of tree-level in $1/(R\ell^{-1})$ series.

2.2 Finite Volume Spectrum of Closed Flux Tubes via Worldsheet Scattering

The analysis of the closed flux tube spectrum employs a refined perturbative framework that unfolds in two distinct stages. Initially, phonon scattering amplitudes are systematically computed within the worldsheet effective theory, utilizing the expansion parameter $p\ell_s$ in the small-momentum regime. Subsequently, these scattering amplitudes are connected to the finite volume spectrum, allowing for potential non-perturbative extensions.

At tree level, phonon interactions exhibit integrability, characterized by a uniform two-body scattering phase shift $e^{2i\delta(s)} = e^{is\ell_s^2/4}$, where s represents the Mandelstam invariant. This enables the application of the TBA formalism to obtain an exact description of the finite volume spectrum.

Higher-order corrections up to $O(\ell_s^4)$ preserve the absence of particle production, with the scattering phase shifts for the symmetric (tensor $2^{\pm}$), antisymmetric (pseudoscalar 0^{--}), and singlet (scalar 0^{++}) channels given by the expressions $2\delta_{\text{sym}} = \frac{\ell_s^2 s}{4} - \frac{11\ell_s^4 s^2}{192\pi} + O(s^3)$, $2\delta_{\text{anti}} = \frac{\ell_s^2 s}{4} + \frac{11\ell_s^4 s^2}{192\pi} + O(s^3)$, $2\delta_{\text{sing}} = \frac{\ell_s^2 s}{4} + \frac{11\ell_s^4 s^2}{192\pi} + O(s^3)$. The leading term in these expressions aligns with the tree-level integrable phase shift, whereas the subleading term captures one-loop scattering effects and remains universal up to this order.

In the helicity basis, defined by $a^\dagger_{l(r)\pm} = a^\dagger_{l(r)2} \pm i a^\dagger_{l(r)3}$, where $a^\dagger_{l(r)}$ represent left- and right-moving phonon creation operators, the scalar and pseudoscalar channels exhibit identical one-loop phase shifts. This feature results in a reflection-free scattering process.

The TBA framework applied to massless, reflectionless excitations enforces quantization conditions around a circular topology in the form

$$\begin{aligned} \epsilon_l^a(q) &= q + \frac{i}{R}\sum_i 2\delta_{ab_i}(q,-ip_{ri}) + \frac{1}{2\pi R}\sum_b \int_0^\infty dq' \frac{d2\delta_{ab}(q,q')}{dq'} \ln\left(1-e^{-R\epsilon_r^b(q')}\right), \\ \epsilon_r^a(q) &= q - \frac{i}{R}\sum_i 2\delta_{b_i a}(q,ip_{li}) + \frac{1}{2\pi R}\sum_b \int_0^\infty dq' \frac{d2\delta_{ba}(q,q')}{dq'} \ln\left(1-e^{-R\epsilon_l^b(q')}\right), \end{aligned} \tag{7}$$

where a_i, a_j index left and right-moving excitations, while b labels all particle types in the $(1+1)$-dimensional system.

Neglecting winding corrections simplifies the TBA equations to the Asymptotic Bethe Ansatz (ABA), effectively summing up classical non-linearities. Under these conditions, the TBA formulation yields the GGRT spectrum as a leading-order result, successfully modeling many string

states. Incorporating higher-order corrections into the full TBA system presents technical challenges, though their impact on winding terms is exponentially suppressed at high momenta, often justifying their omission.

For instance, in a two-phonon scenario, pseudoenergies simplify to a linear form $\epsilon^1_{l(r)}(q) = \epsilon^2_{l(r)}(q) = c_{l(r)}q$, leading to the reduced TBA equations $c_l = 1+\frac{p_r\ell_s^2}{R}-\frac{\pi\ell_s^2}{6c_rR^2}, \quad c_r = 1+\frac{p_l\ell_s^2}{R}-\frac{\pi\ell_s^2}{6c_lR^2}$, and the corresponding energy expression $\Delta E = p_l + p_r - \frac{\pi}{6Rc_l} - \frac{\pi}{6Rc_r}$.

Numerical solutions of the full TBA system confirm the limited ultraviolet sensitivity of winding corrections. Furthermore, these equations facilitate the extraction of scattering phase shifts as functions of p_l, p_r, derived from the two-phonon excitation spectrum of a confining flux tube. This methodology provides a robust foundation for understanding the finite volume spectrum of closed flux tubes in various physical settings.

2.3 The Axionic String Ansatz (ASA)

The universal predictions derived from the TBA framework provide an accurate characterization of a broad range of excitation states in confining strings, as verified with high precision in both $D = 4$ and $D = 3$ spacetime dimensions [15–18]. A general trend observed is that most energy levels exhibit growing deviations from these theoretical predictions as the string length R decreases, indicating the presence of non-universal effects. Particularly, TBA methods facilitate the extraction of the first non-trivial Wilson coefficient for confining strings in $D = 3$ [19, 20].

However, in $D = 4$, certain states display considerable deviations from the expected universal TBA results even for relatively large values of R. This anomaly suggests the existence of an additional massive degree of freedom propagating on the worldsheet, commonly referred to as the worldsheet axion [1, 19].

The interaction of this pseudoscalar axion with the transverse Goldstone bosons at leading order is described by the action:

$$S_\phi = \int d^2\sigma\sqrt{-h}\left(-\frac{1}{2}(\partial\phi)^2 - \frac{1}{2}m^2\phi^2 + \frac{Q_\phi}{4}h^{\alpha\beta}\epsilon_{\mu\nu\lambda\rho}\partial_\alpha t^{\mu\nu}\partial_\beta t^{\lambda\rho}\phi\right) \tag{8}$$

where ϕ represents the pseudoscalar axion field living on the string worldsheet, while the tensor quantity $t^{\mu\nu}$ is given by $t^{\mu\nu} = \frac{\epsilon^{\alpha\beta}}{\sqrt{-h}}\partial_\alpha X^\mu \partial_\beta X^\nu$.

The parameters governing the axion dynamics, specifically the coupling constant Q_ϕ and the axion mass m, can be determined through Monte Carlo simulations of $SU(N_c)$ Yang-Mills theories in $D = 4$. Utilizing TBA techniques for the most precise $SU(3)$ calculation, these parameters have been estimated: $Q_\phi \approx 0.38 \pm 0.04, \quad m \approx 1.85^{+0.02}_{-0.03}\ell_s^{-1}$. Notably, this value of the coupling constant is in close agreement with the integrable theory prediction for $D = 4$ Goldstone bosons coupled to a massless axion [21], given by $Q_{\text{integrable}} = \sqrt{7/16\pi} \approx 0.373$. This alignment suggests a deeper underlying structure governing the interaction between the axion and the string modes.

3. Closed string spectrum via the Thermodynamic Bethe Ansatz

3.1 Quantum Numbers and the closed flux tube spectrum

Before describing the spectrum of excited string states, we first outline their relevant quantum numbers. We consider a closed confining flux tube in the fundamental representation of $SU(N_c)$,

winding around the compactified x-direction, known as a torelon. These states are characterized by several quantum numbers: the transverse momentum $p_\perp = (p_y, p_z)$, which we set to zero since it does not add new insights; the longitudinal momentum $p = 2\pi q/L_x$, with states labeled by $q \geq 0$; the angular momentum J, which takes values $J = 0, \pm 1, \ldots$ and remains symmetric under sign reversal; the transverse parity $P_\perp$, defined as a reflection in the transverse plane, which combines with $J > 0$ states into $O(2)$ doublets; and the longitudinal parity $P_\parallel$, acting as a reflection along the flux tube and linked to the CP parity of the gauge theory, which does not define eigenstates for $q > 0$ due to momentum flipping. We denote the quantum numbers as $|J|^{P_\perp P_\parallel}$ for $q = 0$ states and $(q, |J|^{P_\perp})$ for $q > 0$ states.

Below a computation of the low-lying flux tube spectrum in $D = 4$ Yang-Mills theory [22] using the TBA framework, supplemented by $T\bar{T}$ deformation techniques is presented. The theoretical predictions are systematically compared with lattice results. The analysis confirms that all accessible low-energy excitations of the confining flux tube observed in lattice simulations can be accurately described by an effective long-string theory incorporating a single massive pseudoscalar degree of freedom, with no additional low-energy matter content.

More specifically, the spectrum corresponding to string states with massive excitations and up to two phonon excitations is derived analytically. This is achieved through calculations that employ $2 \to 2$ phonon scattering phase shifts extracted from a proposed effective action. The phase shifts are determined by fitting a minimal set of parameters, ensuring a robust and predictive framework.

For the numerical analysis, the gauge group $SU(3)$ is considered at a choice of β which provides the highest statistical precision for highly excited states. Notably, the data indicates that variations in the number of colors, N_c, as well as in lattice spacing, have a negligible impact on the conclusions.

3.2 Zero Longitudinal Momentum and the Worldsheet Axion

The absolute ground state of the confining flux tube, characterized by the quantum numbers 0^{++}, remains devoid of phonon excitations and is well-described by the GGRT spectrum, along with the expansion in ℓ_s/R. This state facilitates the determination of the string tension via the GGRT formula. Notable deviations from GGRT predictions emerge in the ground states of the 0^{--}, 2^{++}, and 2^{-+} sectors, as well as in the first excited state of the 0^{++} sector, with the most pronounced discrepancies observed in the 0^{--} sector. These deviations can be effectively accounted for through the framework of effective string theory, incorporating a massive pseudoscalar field. This pseudoscalar acts as a resonance on the string worldsheet, influencing phase shifts in phonon scattering and modifying the energy spectrum of excited states. The resonance introduces two key fitting parameters: the mass and the axion coupling, with a fitting procedure yielding $m = 1.812(16)\ell_s^{-1}$ and $Q_\phi = 0.365(5)$. While theoretical predictions demonstrate strong agreement with lattice data, systematic errors, particularly in spin-2 states, affect the accuracy of the fits. The pseudoscalar induces a massive resonance in the 0^{--} sector, contributing to a splitting in both the 0^{++} and spin-2 states. The mass exhibits a weak dependence on N_c with $m = 1.65(2)\ell_s^{-1}$ for $SU(6)$, while the axion coupling remains largely invariant with respect to N_c; see Ref. [22]. Lattice data and theoretical predictions, presented in the left panel of Figure 1, suggest that at large string lengths, the energy levels may be overestimated due to an overestimation of heavy states' contributions. Conversely, deviations at short string lengths may stem from lattice artifacts rather than deficiencies in the EST.

The pseudoscalar is a metastable excitation on the string worldsheet, allowing for the construction of higher excited states. These states are not independent of the GGRT spectrum but can instead be described through a substitution rule. Their energy levels can be approximated using the $T\bar{T}$ dressing approach. The analysis of higher excited states, particularly the first excited state in the 0^{--} sector, is supported by precise numerical data, as illustrated in the right panel of Figure 1.

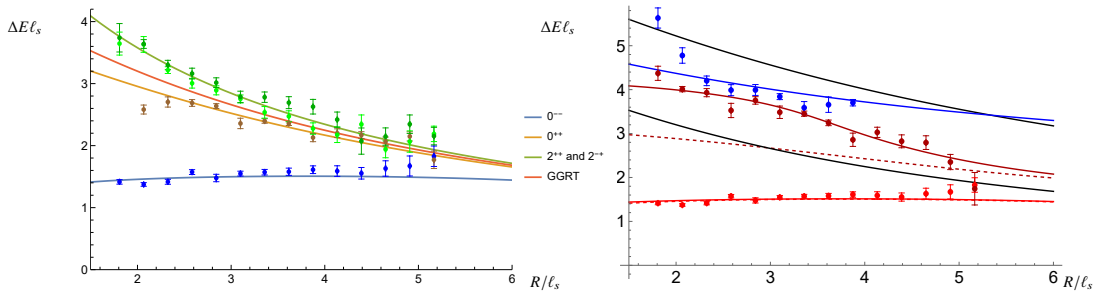

Figure 1: Left Panel: Energy levels at $N_L = N_R = 1$. Solid lines correspond to theoretical predictions for two-phonon excitations derived from the $2 \to 2$ phonon scattering channels: anti-symmetric (blue), singlet (brown), and symmetric (green), incorporating a massive pseudoscalar field via $T\bar{T}$ deformation. Light green and dark green dots denote 2^{++} and 2^{-+} states, respectively. Right Panel: Energy levels of the ground state (bright red), first excited state (dark red), and second excited state (blue) as a function of string length R in the 0^{--} sector. Energies are adjusted by subtracting the linear contribution, $\Delta E = E - R/\ell_s^2$.

This methodology is further applied to higher excited states, particularly the first excited state in the 0^{--} sector. The state, represented by dark red dots in the right panel of Figure 1, can be computed using TBA. However, higher-order corrections become necessary due to the increased phonon momenta. By employing an expansion of the phase shift up to order $s^4\ell_s^{-8}$, a more accurate fit for the spectrum is achieved, as indicated by the darker red solid line in contrast to the dashed line. Additionally, within the 0^{--} sector, another state is observed below the GGRT level $N_L = N_R = 2$. This state, computed via the ABA and $T\bar{T}$ dressing equations, is represented by blue dots in the right panel of Figure 1. The $T\bar{T}$ dressing provides a good description, with deviations at short string lengths likely attributable to higher-order corrections in the phase shift.

An intriguing aspect of the 0^{++} sector is the presence of a second excited state composed of two axions. As depicted in Figure 2, the second excited state (blue dots) aligns well with the predicted energy of two massive excitations after applying $T\bar{T}$ deformation (solid blue line). For comparison, the dashed blue line represents the scenario of free axions. This alignment suggests that the interaction between pseudoscalars is substantial and effectively captured by the $T\bar{T}$ deformation, particularly for short strings. The axion-axion interaction appears to be repulsive.

3.3 Spectrum of the $q = 1$ Flux Tube and Axion Dynamics

This section presents an analysis of the flux tube spectrum in the $q = 1$; 0^- sector, illustrated in the left panel of Figure 3. The ground state, represented by red dots, can be interpreted either as a boosted $2 \to 2$ phonon scattering process in the pseudoscalar channel or as a boosted massive string excitation. These interpretations are modeled using the ABA and $T\bar{T}$ deformations, depicted by solid and dot-dashed red lines, respectively. Both approaches provide a reliable prediction for the ground state, with the two-phonon interpretation exhibiting slightly better accuracy.

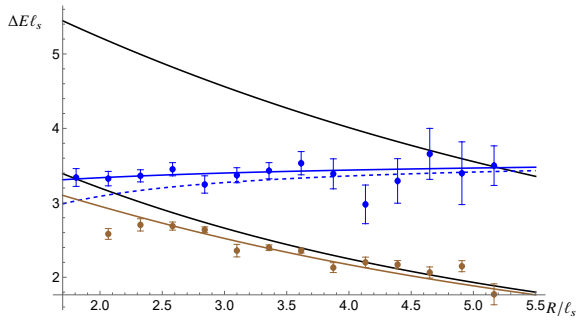

Figure 2: First and second excited states in the 0^{++} sector with $q = 0$, denoted by brown and blue dots, respectively. The solid and dashed blue lines correspond to predictions for two massive excitations with and without $T\bar{T}$ deformation. Black lines indicate GGRT spectra at levels $N_L = N_R = 1$ and $N_L = N_R = 2$, while the brown line represents the GGRT prediction for the $N_L = N_R = 1$ state, incorporating the axionic contribution to the phase shift.

The first excited state, identified as a two-phonon excitation with quantization condition $N_L = 3, N_R = 2$, initially demonstrates poor agreement with theoretical expectations (solid blue line), likely due to significant higher-order corrections at large phonon momenta. Upon incorporating these corrections (dashed lines), predictions for the ground state remain unaffected, whereas the agreement for the first excited state improves considerably.

In the $q = 1$; $1^{\pm}$ sector, illustrated in the right panel of Figure 3, numerical data reveals the presence of three distinct states. The ground and second excited states, represented by black dots, exhibit strong agreement with the predictions of the GGRT model (black lines), with minor deviations potentially arising from high-momentum corrections. The first excited state, shown by red dots, aligns well with ABA and $T\bar{T}$ deformation predictions (solid red line). The $T\bar{T}$ deformation accounts for an attractive axion-phonon interaction; however, it tends to underestimate numerical data for longer strings due to systematic uncertainties. For short strings, predictions derived from the $T\bar{T}$ deformation remain highly accurate.

Regarding spin-2 states in the $q = 1$ sector, numerical data is available only for the ground state, which corresponds to the GGRT state with quantization numbers $N_L = 2, N_R = 1$.

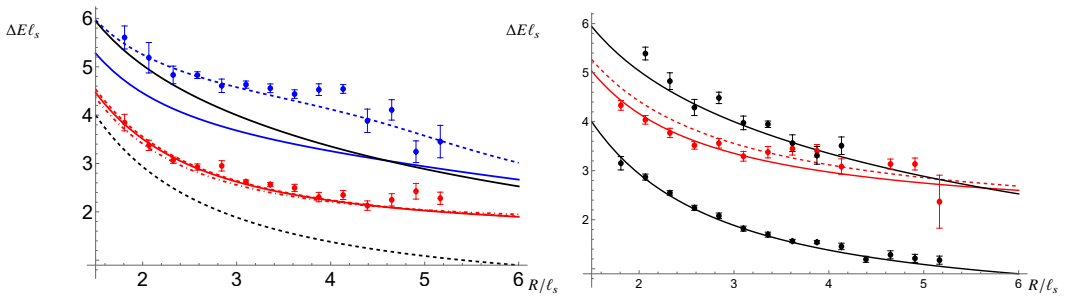

Figure 3: Left Panel: The ground state (red) and first excited state (blue) within the $q = 1$; 0^- sector. Right Panel: The three lowest states in the $q = 1$; $1^{\pm}$ sector. Black dots represent the ground and second excited states, which are in agreement with GGRT spectra. Red dots denote the first excited state, with theoretical predictions depicted using solid and dashed lines.

4. The spectrum of Open Flux Tubes

4.1 The quantum numbers of the open flux tube

The energy levels of an open flux tube can be classified irreducibly using three fundamental quantum numbers. The first quantum number, denoted as Λ, corresponds to the projection of the total angular momentum J onto the axis connecting the quark and antiquark. Different values of Λ are labeled using Greek letters: Σ for $\Lambda = 0$, Π for $\Lambda = 1$, Δ for $\Lambda = 2$, and so on [23].

Another quantum number, η_{CP}, emerges from the combination of charge conjugation (C) and parity inversion ($\mathcal{P}$) about the midpoint of the flux tube. The combined operator, often denoted as $C o \mathcal{P}$, yields eigenvalues that determine whether a state is symmetric (g) or antisymmetric (u). These eigenvalues take values of $+1$ and -1, respectively.

For states with $\Lambda = 0$, an additional quantum number ϵ is introduced, representing the eigenvalue of the reflection operator with respect to any plane containing the charge axis. This reflection symmetry classifies states as either even (+) or odd (−).

By utilizing these symmetries, the open flux tube states are systematically categorized into groups such as Σ_g^+, Σ_g^-, Σ_u^+, Σ_u^-, Π_g, Π_u, Δ_g, Δ_u, and so forth. This classification scheme provides a structured framework for understanding the spectrum of open flux tubes and analyzing their associated gluonic excitations.

4.2 Results for the open flux tube

This section presents the findings related to the spectra of the open flux tube for $N_c = 6$, the highest value of N_c considered in the study [24], across eight irreducible representations: Σ_g^+, Σ_g^-, Σ_u^+, Σ_u^-, Π_g, Π_u, Δ_g, and Δ_u. The corresponding spectra for these representations are illustrated in Figure 4. Results are provided for two different lattice spacings to assess whether the spectral behavior changes as the continuum limit is approached.

The absolute ground state is associated with the Σ_g^+ representation, which closely follows the Arvis potential with a remarkable precision. This ground state corresponds to the vacuum state $|0\rangle$, devoid of phonon excitations, signifying the absence of scattering processes along the string's worldsheet. Consequently, the expectation is that the spectrum aligns well with predictions from the Nambu-Goto model, and thus the Arvis potential.

The lowest excited state observed in the spectrum corresponds to the ground state of the Π_u representation, depicted in orange in the third row from the top and second column. This state exhibits substantial agreement with the Nambu-Goto state characterized by $N = 1$, implying the presence of a single phonon carrying one unit of momentum. Given the absence of scattering processes along the worldsheet, this outcome is unsurprising.

As the analysis extends to higher excited states, an increasing number of deviations from the Nambu-Goto behavior become apparent. Notably, a striking pattern emerges in the ground state of Σ_g^-, as well as throughout the entire spectrum of states associated with Σ_u^-. These states display behavior resembling that of a ground state with an additional constant mass term, as shown in Figure 4. This phenomenon is consistent with theoretical expectations for an axion coupled to the string. Plots presented in Fig.9 in Ref. [24] further emphasize the presence of axion states within these open flux tubes, with the lightest axion state possessing a mass identical to that observed in the spectra of closed flux tubes.

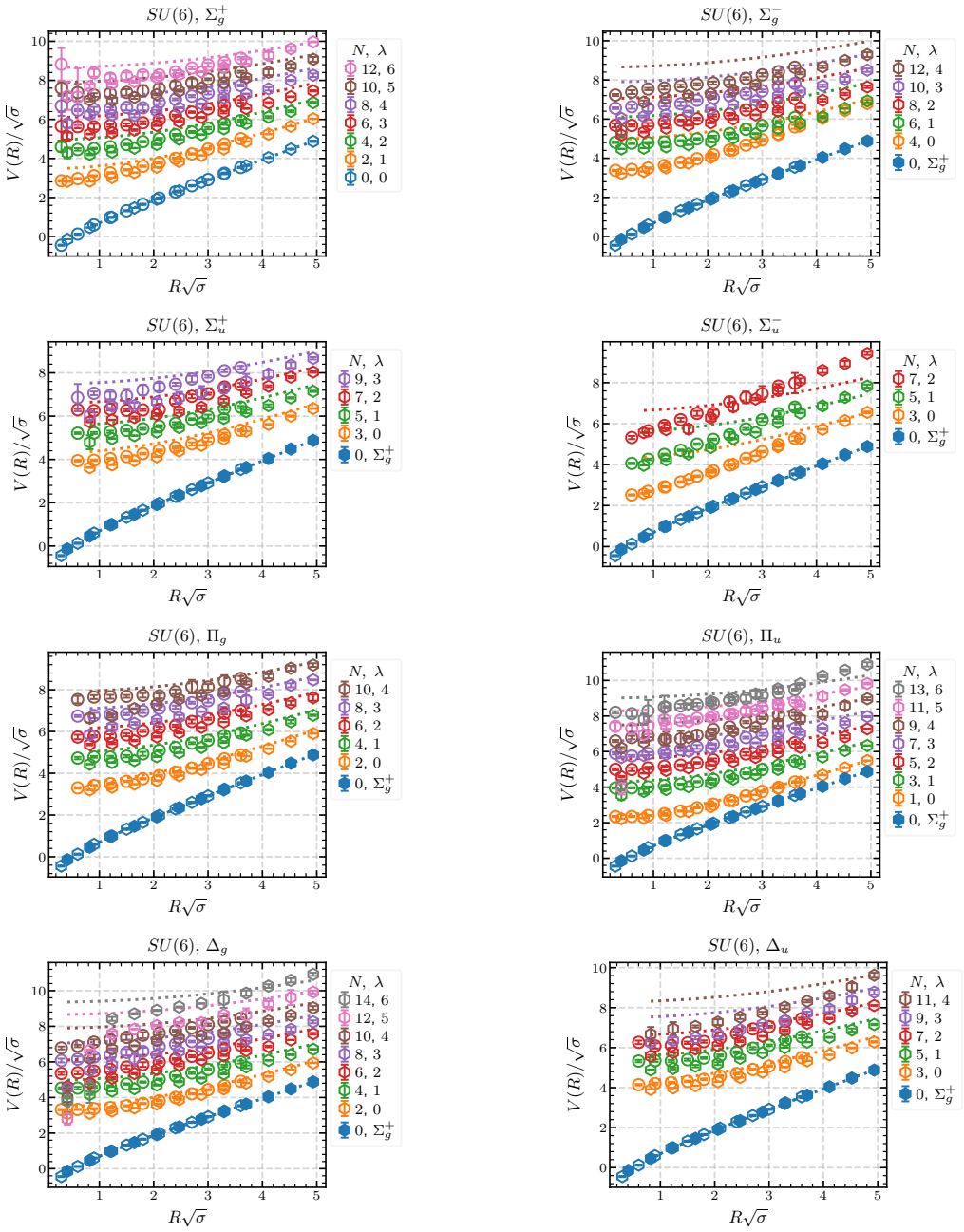

Figure 4: The spectra of eight irreducible representations for $SU(6)$ and two values of the lattice spacing. Namely, polygonal shapes in each figure show the results at coarse lattice, while circle markers indicate finer lattices. N is the quantum number as defined in Eq. 3, and λ is the excitation number.

The lightest axionic signature emerges in the Σ_u^- channel, whose quantum numbers align with those of the axion in the closed flux tube setup 0^{--}. The corresponding mass, $m \sim 1.66\ell_s^{-1}$, is in good agreement with the axion mass found for the closed flux tube, reflecting the fact that the axion is an intrinsic property of the string worldsheet.

5. Conclusions

High-precision computations of the closed confining string spectrum show strong agreement with the theoretical predictions of the Thermodynamic Bethe Ansatz, which incorporate the low-energy effective string action along with a low-mass worldsheet axion. The application of the $T\bar{T}$ deformation to describe interactions confirms the absence of additional low-lying resonances on the string worldsheet within the explored energy range. However, certain challenges remain unresolved, particularly the need for a systematic approach to compute spectra involving three or more phonon excitations. Developing such a framework would facilitate the disentanglement of multi-phonon states and enable the extraction of non-universal Wilson coefficients relevant to 4D QCD flux tubes. Moreover, further support for the Axionic String Ansatz was found, as no evidence of additional resonances was observed.

Recent studies have extended partially this analysis to the spectrum of the open flux tube across various discrete irreducible representations and a wide range of excitation levels. Specifically, the spectrum was extracted for $SU(N_c)$ gauge theories with N_c ranging from 3 to 6. The results indicate minimal finite lattice spacing effects and negligible dependence on N_c, suggesting that the observed physics closely approximates both the large-N_c limit and the continuum.

The analysis further reveals that many states in the low-lying spectrum of the open flux tube can be well described by the Nambu-Goto string model with moderate corrections. However, several states exhibit substantial deviations from Nambu-Goto behavior, displaying characteristics consistent with massive excitations. In particular, a number of massive "axionic" excitations were identified, with the lightest state exhibiting a mass comparable to its counterpart in the closed flux tube. These findings underscore the necessity of developing a TBA-based analysis for the open flux tube, analogous to what has been successfully implemented for the closed flux tube.

References

[1] S. Dubovsky, R. Flauger and V. Gorbenko, *Evidence from Lattice Data for a New Particle on the Worldsheet of the QCD Flux Tube*, *Phys. Rev. Lett.* **111** (2013) 062006 [1301.2325].

[2] A. Athenodorou and M. Teper, *The torelon spectrum and the world-sheet axion*, *PoS* **LATTICE2021** (2022) 103 [2112.11213].

[3] P. Goddard, J. Goldstone, C. Rebbi and C.B. Thorn, *Quantum dynamics of a massless relativistic string*, *Nuclear Physics B* **56** (1973) 109.

[4] J. Arvis, *The exactqq¯ potential in nambu string theory*, *Physics Letters B* **127** (1983) 106.

[5] J. Arvis, *The exact $q\bar{q}$ potential in nambu string theory*, *Phys. Lett. B* **127** (1983) 106.

[6] M. Lüscher, K. Symanzik and P. Weisz, *Anomalies of the free loop wave equation in the WKB approximation*, *Nucl. Phys. B* **173** (1980) 365.

[7] J. Polchinski and A. Strominger, *Effective string theory*, *Phys. Rev. Lett.* **67** (1991) 1681.

[8] M. Luscher and P. Weisz, *String excitation energies in SU(N) gauge theories beyond the free-string approximation*, *JHEP* **07** (2004) 014 [hep-th/0406205].

[9] H.B. Meyer, *Poincare invariance in effective string theories*, *JHEP* **05** (2006) 066 [hep-th/0602281].

[10] O. Aharony and E. Karzbrun, *On the effective action of confining strings*, *JHEP* **06** (2009) 012 [0903.1927].

[11] J.M. Drummond, *Universal subleading spectrum of effective string theory*, hep-th/0411017.

[12] N.D. Hari Dass, P. Matlock and Y. Bharadwaj, *Spectrum to all orders of Polchinski-Strominger Effective String Theory of Polyakov-Liouville Type*, 0910.5615.

[13] O. Aharony and M. Field, *On the effective theory of long open strings*, *JHEP* **01** (2011) 065 [1008.2636].

[14] O. Aharony and N. Klinghoffer, *Corrections to Nambu-Goto energy levels from the effective string action*, *JHEP* **12** (2010) 058 [1008.2648].

[15] A. Athenodorou, B. Bringoltz and M. Teper, *Closed flux tubes and their string description in D=3+1 SU(N) gauge theories*, *JHEP* **02** (2011) 030 [1007.4720].

[16] A. Athenodorou, B. Bringoltz and M. Teper, *Closed flux tubes and their string description in D=2+1 SU(N) gauge theories*, *JHEP* **05** (2011) 042 [1103.5854].

[17] A. Athenodorou and M. Teper, *On the spectrum and string tension of U(1) lattice gauge theory in 2 + 1 dimensions*, *JHEP* **01** (2019) 063 [1811.06280].

[18] A. Athenodorou, S. Dubovsky, C. Luo and M. Teper, *Excitations of Ising strings on a lattice*, *JHEP* **05** (2023) 082 [2301.00034].

[19] S. Dubovsky, R. Flauger and V. Gorbenko, *Flux Tube Spectra from Approximate Integrability at Low Energies*, *J. Exp. Theor. Phys.* **120** (2015) 399 [1404.0037].

[20] C. Chen, P. Conkey, S. Dubovsky and G. Hernández-Chifflet, *Undressing Confining Flux Tubes with $T\bar{T}$*, *Phys. Rev. D* **98** (2018) 114024 [1808.01339].

[21] S. Dubovsky and V. Gorbenko, *Towards a Theory of the QCD String*, *JHEP* **02** (2016) 022 [1511.01908].

[22] A. Athenodorou, S. Dubovsky, C. Luo and M. Teper, *Confining Strings and the Worldsheet Axion from the Lattice*, 2411.03435.

[23] J. Kuti, *Lattice QCD and string theory*, *PoS* **LAT2005** (2006) 001 [hep-lat/0511023].

[24] A. Sharifian, A. Athenodorou and P. Bicudo, *The spectrum of open confining strings in the large-N_c limit*, *PoS* **LATTICE2024** (2025) 467 [2411.07412].